$e^+e^- \rightarrow N\overline{N}$ at BESIII

Marco Maggiora*
on behalf of the BESIII Collaboration

* Department of Physics, University of Turin and INFN, Turin

Electromagnetic structure of hadrons: annihilation and scattering processes

GDR 3034 - Chromodynamique Quantique
et Physique des Hadrons

GDR-PH-QCD, Meeting Groupe 2

Orsay, October 3rd - 5th, 2012

BESIII/BEPCII

BEPCII: e^+e^- double ring collider

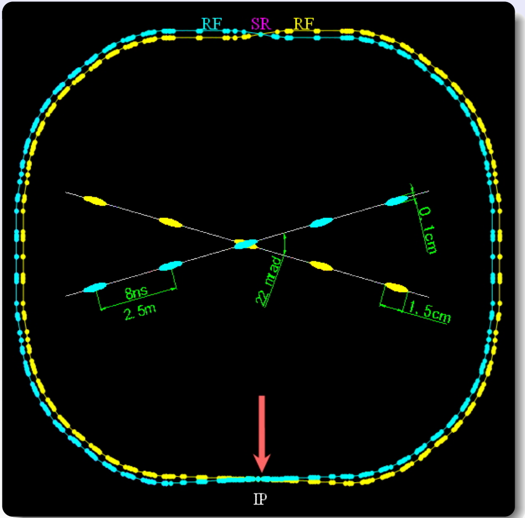

Design Features

- Beam energy: **1.0** - **2.3** GeV
- Crossing angle: **22** mrad (DAΦNE 50 mrad)
- **Luminosity: 10^{33} cm^{-2}s^{-1}**
- **Optimum energy: 1.89 GeV**
- Energy spread: **5.16** $\times$ **10**$^{-4}$
- Number of bunches: **93**
- Bunch length: **1.5** cm
- Total current: **0.91** A

The **BESIII** detector

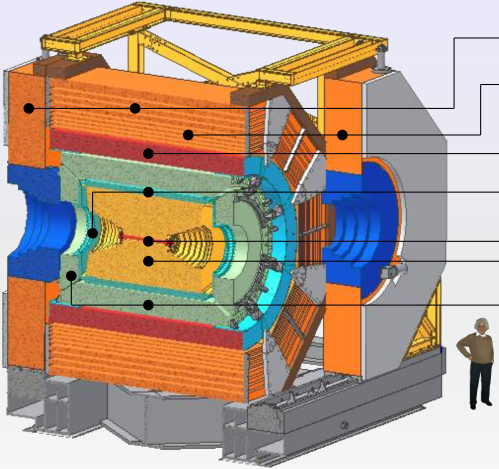

- **Magnet yoke**
- **RPC (9/8 layers Barrel/Endcaps)**
- **SC magnet, 1 Tesla**
- **TOF (scintillators), 90 ps**
- **Be beam pipe**
- **MDC, 120μm**
- **CsI(Tl) calorimeter, 2.5% at 1 GeV**

A significant improvement with respect to BESII

The **BESII** and **BESIII** detectors

BESII @ BEPC

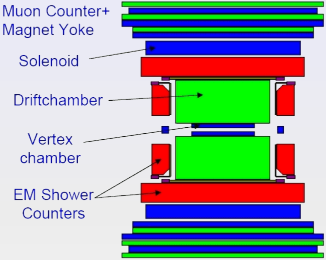

BESIII @ BEPCII

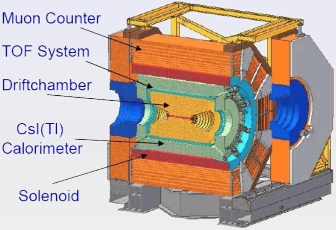

Device	Performance
MDC	$\sigma_p/p = 1.7\%\sqrt{1+p^2}$, $dE/dx = 8\%$
TOF	180 ps (bhabha)
EMC	$\sigma_E/E < 22\%/\sqrt{E}$
MUC	3 layers
Magnet	0.4 T Solenoidal

Device	Performance
MDC	$\sigma_p/p = 0.5\%$, $dE/dx < 6\%$
TOF	80 ps barrel (bhabha), 100 ps endcap
EMC	$\sigma_E/E < 2.5\%/\sqrt{E}$
MUC	9 barrel + 8 endcap layers
Magnet	1 T Solenoidal

- $R_{\rm had}$ **and precision test of Standard Model**
- **Light hadron spectroscopy** ($\phi f_0(980)$, $\phi\pi^0$,...)
- **Charm and charmonium physics**
- τ **physics**
- **Precision measurements of CKM matrix elements**
- **Search for new physics / new particles**

Physics Channels	Energy (GeV)	Luminosity (10^{33} cm^{-2} s^{-1})	Events/year
J/Ψ	3.10	0.6	1.0×10^{10}
τ	3.67	1.0	1.2×10^{7}
$\Psi(2S)$	3.69	1.0	3.0×10^{9}
D^*	3.77	1.0	2.5×10^{7}
D_s	4.03	0.6	1.0×10^{6}
D_s	4.14	0.6	2.0×10^{6}

BEPCII / BESIII milestones

- **Mar. 2008:** Collisions at 500 mA $\times$ 500 mA, Luminosity: 1 $\times$ $10^{32} cm^{-2} s^{-1}$
- **Apr. 30, 2008:** Move BESIII to IP
- **July 18, 2008:** First e^+e^- collision event in BESIII
- **Apr. 14, 2009:** $\sim$ 106 M $\Psi(2S)$ events ($150 pb^{-1}$) $\sim$ 4$\times$CLEO-c ($\sim$ $42 pb^{-1}$ at 3.65 GeV)
- **July 28, 2009:** $\sim$ 225 M J/Ψ events ($65 pb^{-1}$) $\sim$ 4$\times$BESII
- **2010-2011:** $\sim$ $2.9 fb^{-1}$ at $\psi(3770)$ $\sim$ 11$\times$CLEO-c ($\sim$ $70 pb^{-1}$ scanning in the $\psi(3770)$ energy region)
- **May, 2011:** $\sim$ $0.5 fb^{-1}$ at 4.01 GeV (Ds and XYZ spectroscopy)
- **2012:** $\sim$ 0.4 B $\Psi(2S)$ events $\sim$ 16$\times$CLEO-c
  $\sim$ 1 B J/Ψ events $\sim$ 18$\times$BESII

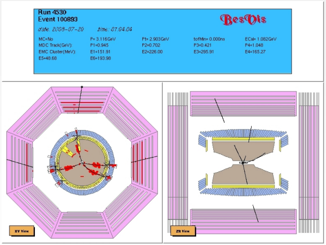

Record Luminosity
6.5 $\times$ $10^{32} cm^{-2} s^{-1}$
or
8 $\times$ CESRc
45 $\times$ BEPC

The ratio $R = \mu_p \frac{G_E^p}{G_M^p}$

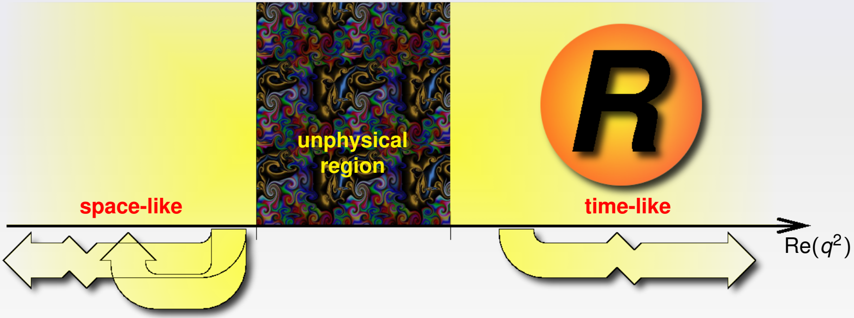

Nucleon form factors and cross sections

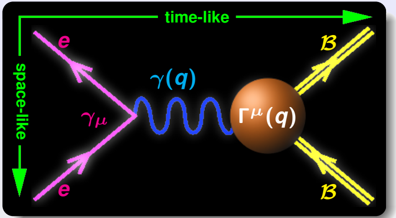

Nucleon current operator (Dirac & Pauli)

$$\Gamma^\mu(q) = \gamma^\mu F_1(q^2) + \frac{i}{2M_{\mathcal{B}}}\sigma^{\mu\nu} q_\nu F_2(q^2)$$

Electric and Magnetic Form Factors

$$G_E(q^2) = F_1(q^2) + \tau F_2(q^2)$$
$$G_M(q^2) = F_1(q^2) + F_2(q^2)$$
$$\tau = \frac{q^2}{4M_{\mathcal{B}}^2}$$

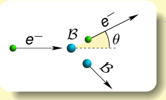

Elastic scattering (Rosenbluth)

$$\frac{d\sigma}{d\Omega} = \frac{\alpha^2 E'_e \cos^2\frac{\theta}{2}}{4E_e^3 \sin^4\frac{\theta}{2}} \left[G_E^2 - \tau\left(1+2(1-\tau)\tan^2\frac{\theta}{2}\right)G_M^2\right]\frac{1}{1-\tau}$$

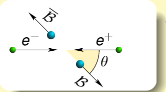

Annihilation

Coulomb correction

$$\frac{d\sigma}{d\Omega} = \frac{\alpha^2 \beta C}{4q^2}\left[(1+\cos^2\theta)|G_M|^2 + \frac{1}{\tau}\sin^2\theta |G_E|^2\right]$$

$$\beta = \sqrt{1-\frac{1}{\tau}}$$

Pointlike fermions e.g. $e^+e^- \to \mu^+\mu^-$: $\frac{d\sigma}{d\Omega} = \frac{\alpha^2 \beta_\mu C}{4q^2}\left(2-\beta_\mu^2 \sin^2\theta\right)$ $\Longrightarrow$ $|G_E| = |G_M| \equiv 1$

Analyticity of baryon form factors

q^2-complex plane

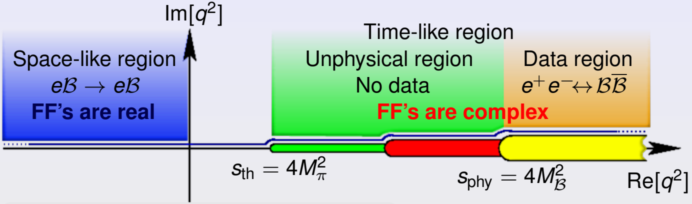

Crossing: tot. helicity $= \begin{cases} 1 \Rightarrow G_E \\ 0 \Rightarrow G_M \end{cases}$

$$G_E(4M_\mathcal{B}^2) = G_M(4M_\mathcal{B}^2)$$

QCD counting rule constrains the asymptotic behaviour

Matveev, Muradyan, Tevkheldize, Brodsky, Farrar

Counting rule: $q^2 \to -\infty$
$i = 1$ **Dirac,** $i = 2$ **Pauli FF**

$$F_i(q^2) \propto (-q^2)^{-(i+1)} \Rightarrow G_{E,M} \propto (-q^2)^{-2}$$

Analyticity: $q^2 \to \pm\infty$
(Phragmèn Lindelöf)

$$G_{E,M}(-\infty) = G_{E,M}(+\infty)$$

G_E^p and G_M^p with Rosenbluth separation

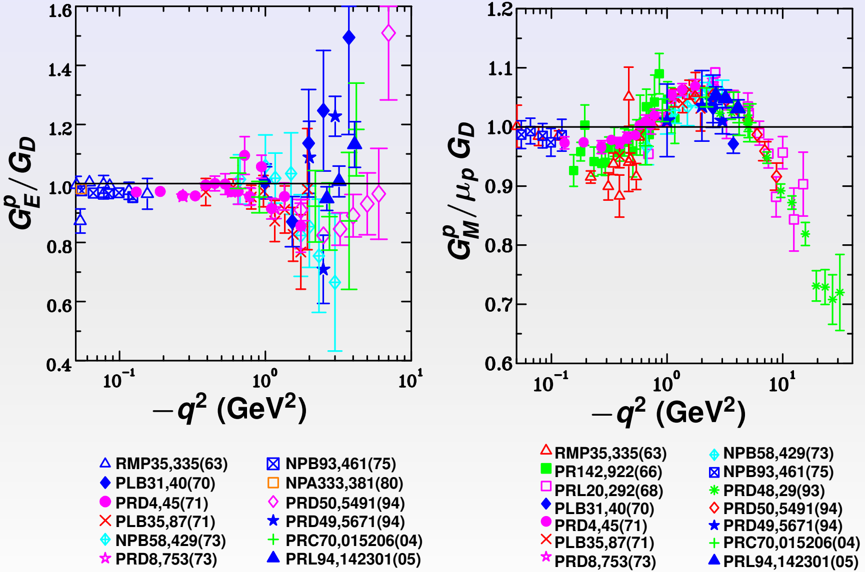

G_E^p/G_M^p in polarization transfer experiments

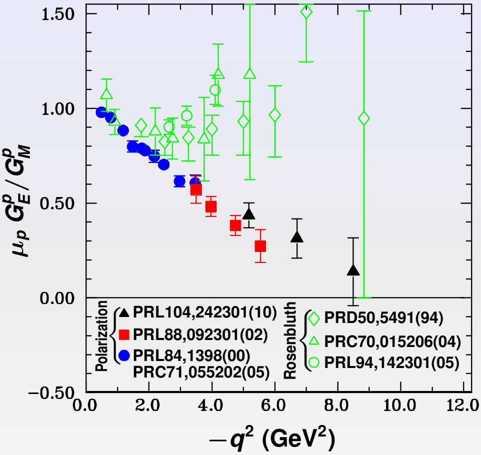

Polarization data do not agree with old Rosenbluth data (◇)

New Rosenbluth separation data from JLab still do not agree with polarization data

G_E^n and G_M^n with different techniques

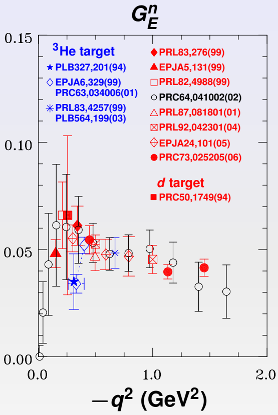

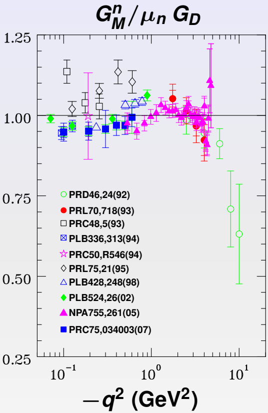

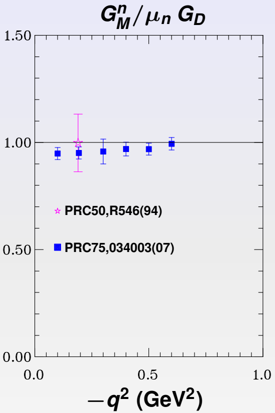

- Elastic *e-d* cross section
- Polarization observables in electron scattering with ^{2}H and ^{3}He targets

- Quasi-elastic *e-d* / elastic *e-p* cross sections
- Polarization observables in electron scattering on a polarized $^3\vec{\text{He}}$ target

RC in Rosenbluth separation: an example

PRD50,5491(94)

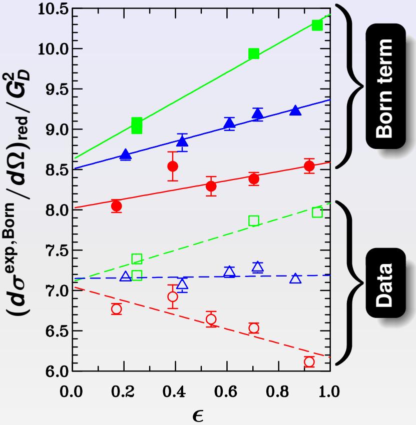

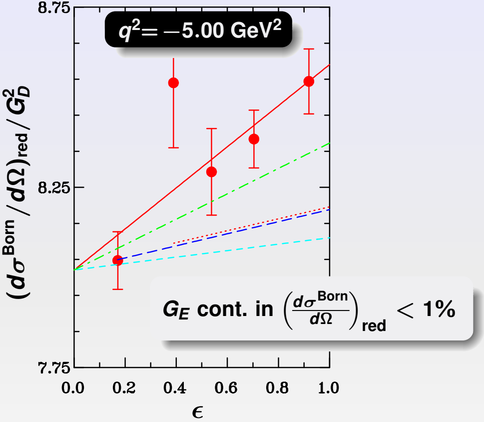

○ ●: $q^2 = -5.00\ \mathrm{GeV}^2$

△ ▲: $q^2 = -3.25\ \mathrm{GeV}^2$

□ ■: $q^2 = -1.75\ \mathrm{GeV}^2$

- Virtual Compton Scattering PRC62,025501(00)
- Two-photon with GPD PRD72,013008(05)
- Structure functions RC (Egle) PRC75,015207(07)
- Polarization data

Rosenbluth $\to$ Polarization

Two-photon exchange (2γ-GPD)

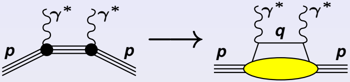

- Two-photon exchange: contributions from intermediate far off-shell states
- Two hard photons
- Structure of nucleon: partonic “handbag” and GPD’s

Structure function radiative corrections (SF-RC)

- Hard bremsstrahlung from electron lines
- No co-linearity approximation
- Two-photon exchange contribution $\sim$ 1%

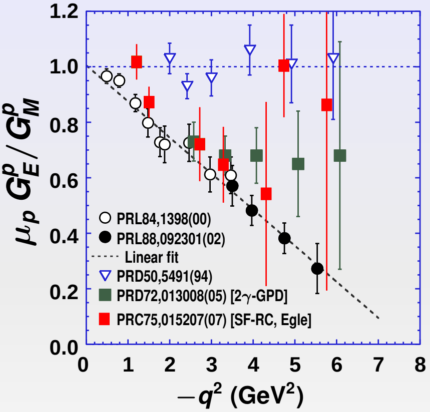

2γ-GPD and SF-RC change the slope in Rosenbluth plots

2γ-GPD and SF-RC have negligible contribution to the polarized cross section ratio

The **1γ-2γ** interference terms have opposite signs in e^+p and e^-p elastic scattering cross sections $\sigma_\pm$

A large (some %) **2γ** contribution produces deviations from unity as a function of ϵ for the ratio σ_+/σ_-

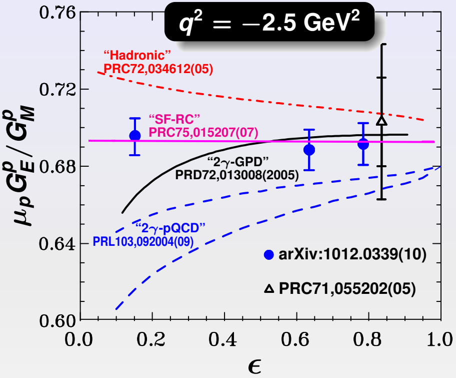

No evidence of two-photon effects

Time-like magnetic proton form factor

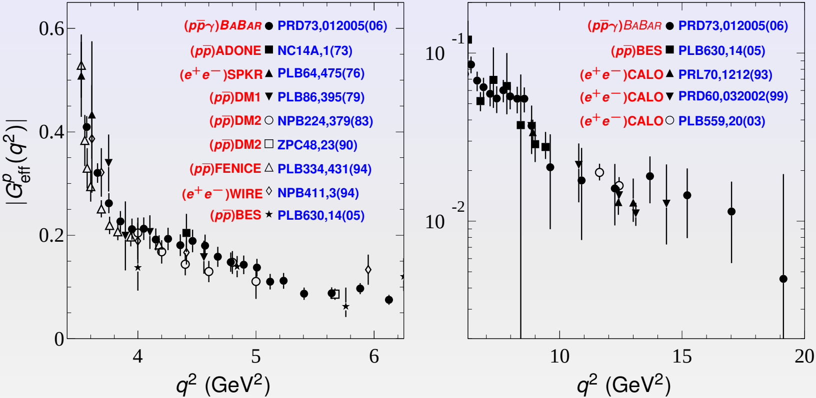

Data obtained assuming $|G^p_M| = |G^p_E| \equiv |G^p_{eff}|$ (true only at threshold)

$$|G^p_{eff}|^2 = \frac{\sigma_{p\bar{p}}(q^2)}{\frac{16\pi\alpha^2 C_e}{3}\,\frac{\sqrt{1-1/\tau}}{4q^2}\left(1+\frac{1}{2\tau}\right)}$$

Asymptotic behavior

E. Tomasi-Gustafsson and M. P. Rekalo, PLB504,291
E. Tomasi-Gustafsson, arXiv:0907.4442

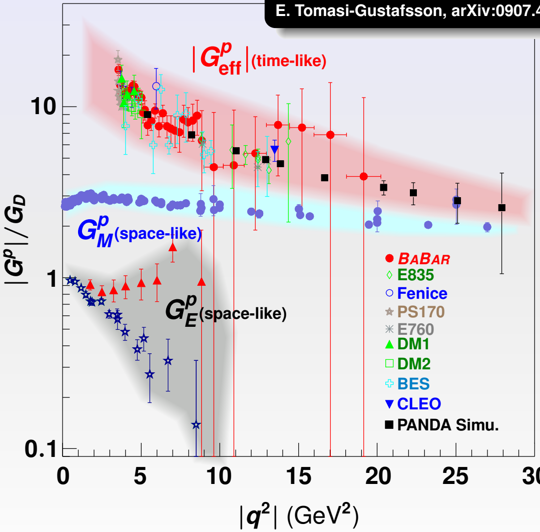

pQCD

$$G^p_{eff}(q^2) \underset{q^2\to\infty}{\sim} G^p_M(q^2)$$

Phragmèn Lindelöf

$$\lim_{q^2\to\infty} \frac{G^p_{eff}(q^2)}{G^p_M(-q^2)} = 1$$

$e^+e^- \to p\bar{p}$ angular distribution (BABAR)

$\cos\theta_p$ distributions form threshold up to 3 GeV [intervals in $E_{CM} \equiv q$ (GeV)]

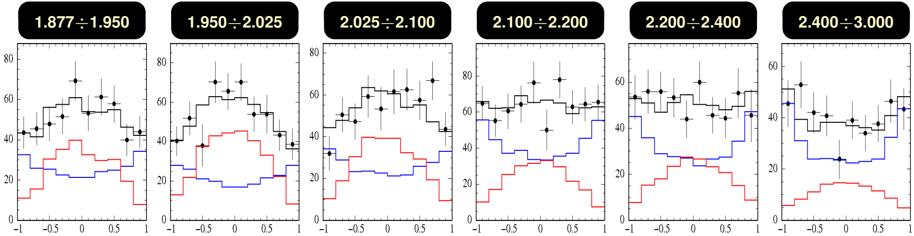

Events/0.2 vs. $\cos\theta_p$

$$\frac{d\sigma}{d\cos\theta_p} = A\left[H_E(\cos\theta_p, q^2)\left|\frac{G_E^p(q^2)}{G_M^p(q^2)}\right|^2 + H_M(\cos\theta_p, q^2)\right]$$

H_E and H_M from MC

Histograms show contributions from

- G_E 
- G_M 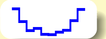

At low q

$\sin^2\theta_p > 1 + \cos^2\theta_p$

$\Rightarrow$

First observation!

$|G_E^p| > |G_M^p|$

At higher q, $|G_E^p| \to |G_M^p|$

Time-like $|G_E^p/G_M^p|$ measurements

$$\frac{d\sigma}{d\cos\theta} = \frac{\pi\alpha^2\beta C}{2q^2}|G_M^p|^2\left[(1+\cos^2\theta)+\frac{4M_p^2}{q^2\mu_p^2}\sin^2\theta|R|^2\right]$$

$$R(q^2) = \mu_p\frac{G_E^p(q^2)}{G_M^p(q^2)}$$

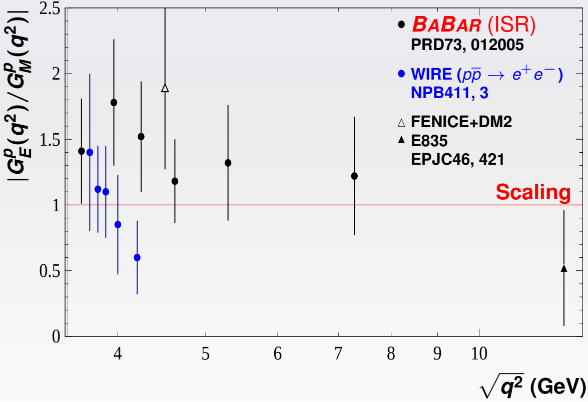

$\gamma\gamma$ exchange

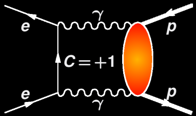

$\gamma\gamma$ exchange interferes with the Born term

Asymmetry in angular distributions

[E. Tomasi-Gustafsson, M.P. Rekalo, PLB504,291(01)]

$\gamma\gamma$ exchange from $e^+e^- \to p\bar{p}\gamma$ BABAR data

E. Tomasi-Gustafsson,
E.A. Kuraev, S. Bakmaev, SP
PLB659,197(08)

$$\mathcal{A}\left(\theta, q^2\right) = \frac{\frac{d\sigma}{d\Omega}\left(\theta, q^2\right) - \frac{d\sigma}{d\Omega}\left(\pi-\theta, q^2\right)}{\frac{d\sigma}{d\Omega}\left(\theta, q^2\right) + \frac{d\sigma}{d\Omega}\left(\pi-\theta, q^2\right)} = \frac{\frac{d\sigma}{d\Omega}\left(\theta, q^2\right) - \frac{d\sigma}{d\Omega}\left(\pi-\theta, q^2\right)}{2\frac{d\sigma^{\text{Born}}}{d\Omega}\left(\theta, q^2\right)}$$

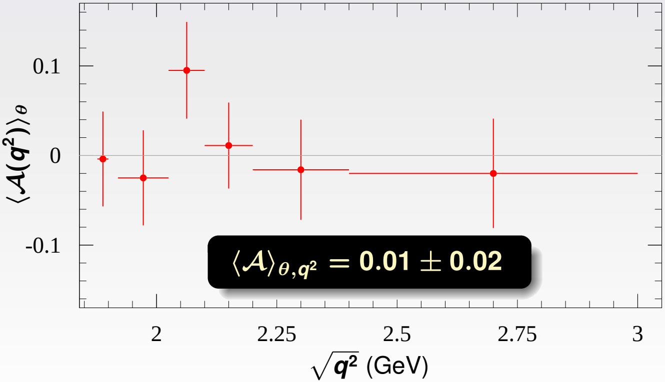

$|G_E^p(q^2)|$ and $|G_M^p(q^2)|$ from $\sigma_{p\bar{p}}$ and DR

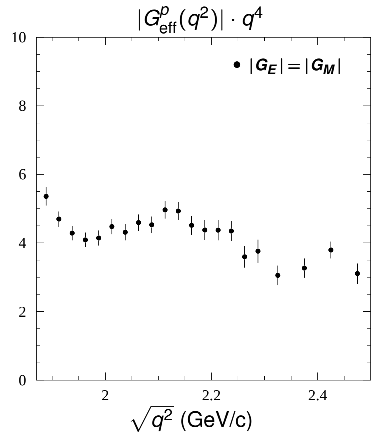

$$|G_{\rm eff}(q^2)|^2 = \frac{\sigma_{p\bar{p}}(q^2)}{\frac{4\pi\alpha^2\beta C}{3s}}\left(1+\frac{1}{2\tau}\right)^{-1}$$

- **Usually what is extracted from the cross section $\sigma(e^+e^- \to p\bar{p})$ is the effective time-like form factor $|G^p_{\rm eff}|$ obtained assuming $|G^p_E| = |G^p_M|$ i.e. $|R| = \mu_p$**
- **Using DR's to parameterize R and the BaBar data on $\sigma(e^+e^- \leftrightarrow p\bar{p})$, $|G^p_E|$ and $|G^p_M|$ may be disentangled**
- **BESIII can measure separately $|G^p_E|$ and $|G^p_M|$**

Cfr. talk by Simone Pacetti

$|G_E^p(q^2)|$ and $|G_M^p(q^2)|$ from $\sigma_{p\bar{p}}$ and DR

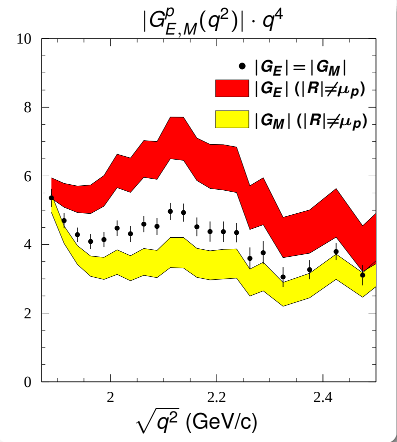

$$|G_M(q^2)|^2 = \frac{\sigma_{p\bar{p}}(q^2)}{\frac{4\pi\alpha^2\beta C}{3s}} \left(1 + \frac{|R(q^2)|}{2\mu_p\tau}\right)^{-1}$$

- **Usually what is extracted from the cross section $\sigma(e^+e^- \to p\bar{p})$ is the effective time-like form factor $|G^p_{\text{eff}}|$ obtained assuming $|G^p_E| = |G^p_M|$ i.e. $|R| = \mu_p$**
- **Using DR's to parameterize R and the BABAR data on $\sigma(e^+e^- \leftrightarrow p\bar{p})$, $|G^p_E|$ and $|G^p_M|$ may be disentangled**
- **BESIII can measure separately $|G^p_E|$ and $|G^p_M|$**

Cfr. talk by Simone Pacetti

Future data on $R = \mu_p G_E^p / G_M^p$

Space-like region

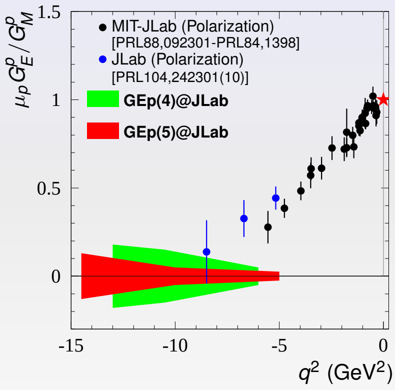

Time-like region

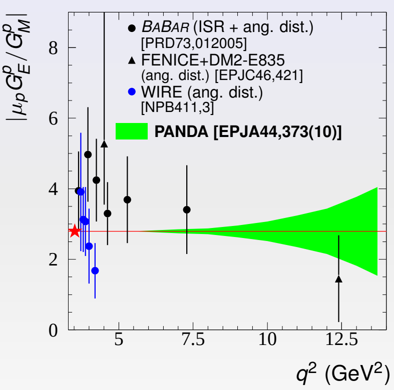

ISR

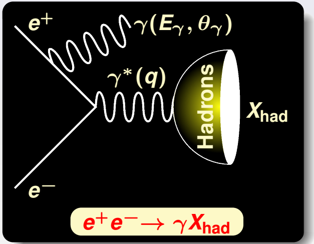

e^+
$\gamma(E_\gamma, \theta_\gamma)$
$\gamma^*(q)$
Hadrons
X_{had}
e^-
$e^+e^- \to \gamma X_{\text{had}}$

ISR: Physics Motivations

- Existing results, obtained by ***BABAR*** (ISR), show interesting and unexpected behaviors, mainly at thresholds, for

$e^+e^- \to p\bar{p}$ and $e^+e^- \to \Lambda\bar{\Lambda}$

- Only one measurement (**FENICE** with energy scan) for

$e^+e^- \to n\bar{n}$

There are physical limits in reaching the threshold of many of these channels via energy scan (stable hadrons produced at rest can not be detected)

The Initial State Radiation technique provides a unique tool to access threshold regions working at higher resonances

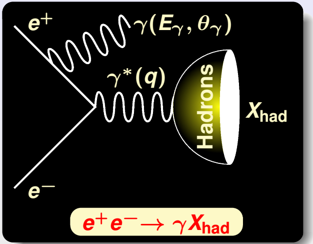

- $$\frac{d^2\sigma}{dE_\gamma d\theta_\gamma} = W(E_\gamma, \theta_\gamma) \cdot \sigma_{e^+e^- \to X_{\text{had}}}(s)$$
- $$W(E_\gamma, \theta_\gamma) = \frac{\alpha}{\pi x}\left(\frac{2 - 2x + x^2}{\sin^2\theta_\gamma}\right)$$

- $s = q^2$, q .... X_{had} momentum
- E_γ, θ_γ ... CM γ energy, scatt. ang.
- E_{CM} .... CM e^+e^- energy
- $x = E_\gamma / 2E_{\text{CM}}$

Advantages

- All energies (q^2) at the same time
  $\Downarrow$
  Better control on systematics
  (e.g. greatly reduced point to point)
- Detected ISR $\Rightarrow$ full X_{had} angular coverage
- CM boost $\Rightarrow$ $\begin{cases}\text{at threshold } \epsilon \neq 0 \\ \text{energy resolution} \sim 1\ \text{MeV}\end{cases}$

ISR Luminosity

$$\frac{dL}{dq} = \frac{2q}{E^2_{cm}} L_{ee} \int_{\cos\theta_\gamma^{min}}^{\cos\theta_\gamma^{max}} W(E_\gamma, \theta_\gamma) d\cos\theta_\gamma$$

L_{ee} .... total luminosity

$\theta_\gamma^{min,\,max}$ ..... geom. accept.

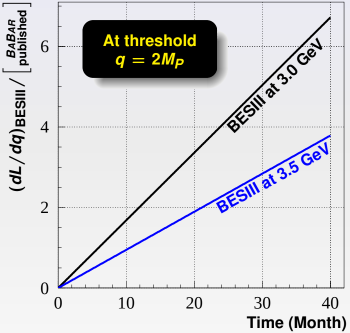

BESIII: lower CM energy ⇒ lower background ⇒ ISR γ detection + 0^o and No ISR γ detection ⇒ $\times$2.5 and $\times$5 in statistics

$$\frac{d^2L}{d\cos\theta_\gamma d\sqrt{s}} = \frac{2\sqrt{s}\,L_{e^+e^-}}{E^2_{c.m.}}\frac{\alpha}{\pi x}\left(\frac{2-2x+x^2}{\sin^2\theta_\gamma} - \frac{x^2}{2}\right)$$

$L_{e^+e^-}$ = luminosity

$$x = \frac{2E_\gamma}{E_{c.m.}} = 1 - \frac{s}{E^2_{c.m.}}$$

- $E^{BABAR}_{c.m.} = 10.58$ GeV
- $E^{BESIII}_{c.m.} = 3.69$ GeV
- $\theta_\gamma \in [20°, 160°]$

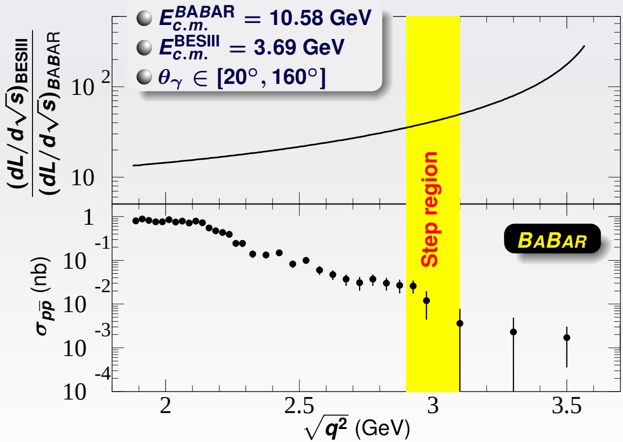

ISR and final state radiation

PRD84,017301

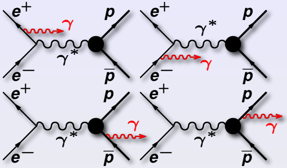

$$\frac{d^2\sigma_{\rm ISR}}{dE_\gamma d\theta_\gamma} = \frac{\alpha^3 E_\gamma}{3E^2_{c.m.}s}\left(|G^p_M(s)|^2 + \frac{|G^p_E(s)|^2}{2\tau}\right)\mathcal{W}(E_\gamma,\theta_\gamma)$$

$$\frac{d^2\sigma_{\rm FSR}}{dE_\gamma d\theta_\gamma} = \frac{\alpha^3 E_\gamma}{3E^4_{c.m.}}\,\mathcal{F}\left[E_\gamma,\theta_\gamma,G^p_E(E^2_{c.m.}),G^p_M(E^2_{c.m.})\right]$$

No ISR-FSR interference after $d\Phi(p\bar{p})$ integration

$$R_{\rm ISR/FSR} = \frac{d\sigma_{\rm ISR}/dE_\gamma}{d\sigma_{\rm ISR}/dE_\gamma + d\sigma_{\rm FSR}/dE_\gamma}\,[20^\circ \le \theta_\gamma \le 160^\circ]$$

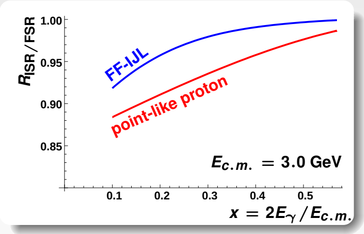

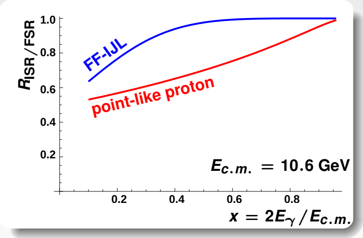

For large values of x or at small angle θ_γ of photon emission the final state radiation is strongly suppressed

ISR angular distribution and zero-degree tagging

ISR angular distribution peaked at low angles

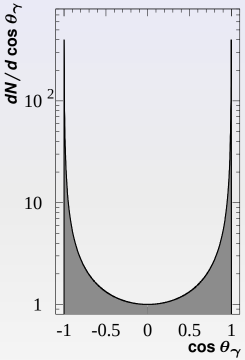

$$\frac{dN}{d\cos\theta_\gamma} = \frac{1-\cos\theta_\gamma^2}{\left(1-\beta_e^2\cos^2\theta_\gamma\right)^2}$$

$$\beta_e = \sqrt{1-4m_e^2/E_{c.m.}^2}$$

$$\Delta N(\theta^{min}) \propto \int_{\theta_\gamma^{min}}^{90^o} d\theta_\gamma \frac{dN}{d\theta_\gamma}$$

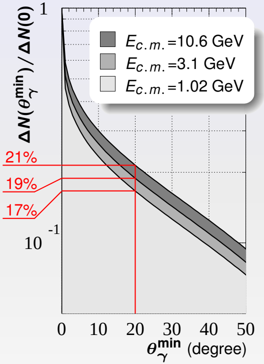

With a typical $\theta_\gamma^{min} = 20^o$
$\sim$ 80% of events is lost!

$$\Delta N(\theta^{max}) \propto \int_0^{\theta_\gamma^{max}} d\theta_\gamma \frac{dN}{d\theta_\gamma}$$

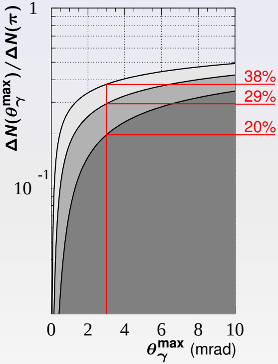

With $\theta^{max} = 3$ mrad more statistics than at wide angle!

BESIII Zero-Degree Detector

- J/Ψ, $\Psi(2S)$, $\psi(3770)$ **resonances decay with high BR's to final states with π^0 and γ_{FS} (final state)**
- **At BESIII these decay channels represent severe backgrounds for typical ISR final states with γ_{IS} detected at wide angle**

- π^0 **and final γ angular distributions are isotropic**
- **ISR angular distribution is peaked at small angles**

$\Longrightarrow$

A zero-degree radiative photon tagger will suppress most of these backgrounds

A new zero-degree detector (ZDD), has been installed on summer 2011 at BESIII to tag ISR photons as well as to measure the luminosity

Pointlike Baryons?

The Coulomb Factor

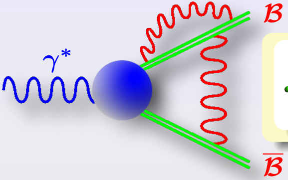

$p\bar{p}$ Coulomb interaction as FSI

[Sommerfeld, Sakharov, Schwinger, Fadin, Khoze]

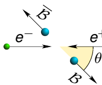

Annihilation **Coulomb correction**

$$\frac{d\sigma}{d\Omega} = \frac{\alpha^2 \beta C}{4q^2}\left[(1+\cos^2\theta)|G_M|^2 + \frac{1}{\tau}\sin^2\theta |G_E|^2\right]$$

Distorted wave approximation

$$C = |\Psi_{\mathrm{Coul}}(0)|^2$$

S-wave: $$C = \frac{\frac{\pi\alpha}{\beta}}{1-\exp\left(-\frac{\pi\alpha}{\beta}\right)} \xrightarrow[\beta\to 0]{} \frac{\pi\alpha}{\beta}$$

D-wave: $C = 1$

No Coulomb factor for boson pairs (P-wave)

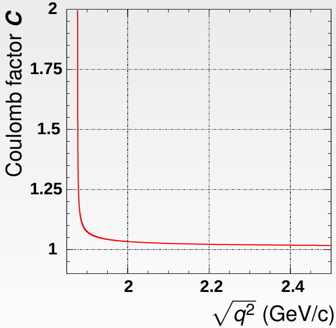

$e^+e^- \to p\bar{p}$

$$\sigma(e^+e^- \to p\bar{p}) = \frac{4\pi\alpha^2\beta_p C}{3q^2}\left[|G_M|^2 + \frac{2M_p^2}{q^2}|G_E|^2\right]$$

$$C \underset{\beta\to 0}{\sim} \frac{\pi\alpha}{\beta}$$

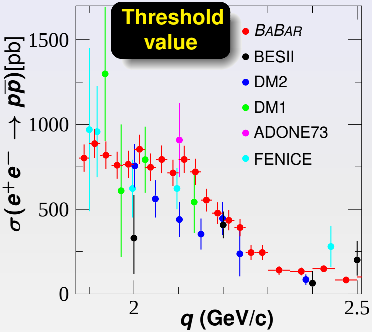

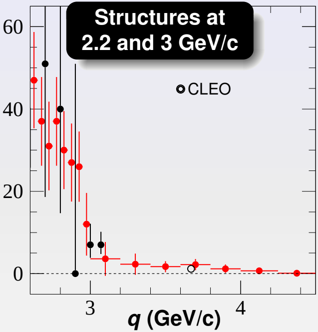

$$\sigma(e^+e^- \to p\bar{p})(4M_p^2) = \frac{\pi^2\alpha^3}{2M_p^2}\frac{\not{\beta_p}}{\not{\beta_p}}|G^p(4M_p^2)|^2 = 0.85\,|G^p(4M_p^2)|^2 \text{ nb}$$

$|G^p(4M_p^2)| \equiv 1$ **as pointlike fermion pairs!**

Using the ISR technique with only few fb^{-1} of integrated luminosity BESIII can easily achieve the *BABAR* statistics

Sommerfeld Enhancement and Resummation Factors

Coulomb Factor $\mathcal{C}$ for S-wave only:

- **Partial wave FF:** $G_S = \frac{2G_M\sqrt{q^2/4M^2} + G_E}{3}$ $G_D = \frac{G_M\sqrt{q^2/4M^2} - G_E}{3}$
- **Cross section:** $\sigma(q^2) = 2\pi\alpha^2\beta\,\frac{4M^2}{(q^2)^2}\left[\mathcal{C}\,|G_S(q^2)|^2 + 2|G_D(q^2)|^2\right]$

$$\mathcal{C} = \mathcal{E} \times \mathcal{R}$$

- **Enhancement factor:** $\mathcal{E} = \pi\alpha/\beta$
- **Step at threshold:** $\sigma_{p\bar{p}}(4M_p^2) = \frac{\pi^2\alpha^3}{2M^2}\frac{\beta}{\beta}|G_S^p(4M_p^2)|^2 = 0.85\,|G_S^p(4M_p^2)|^2$ nb

- **Resummation factor:** $\mathcal{R} = 1/[1 - \exp(-\pi\alpha/\beta)]$
- **Few MeV above threshold:** $\mathcal{C} \simeq 1 \;\Rightarrow\; \sigma_{p\bar{p}}(q^2) \propto \beta\,|G_S^p(q^2)|^2$

BaBar: $e^+e^- \rightarrow p\bar{p}$

Expected cross section with

$|G_S^p(4M_p^2)| = 1$

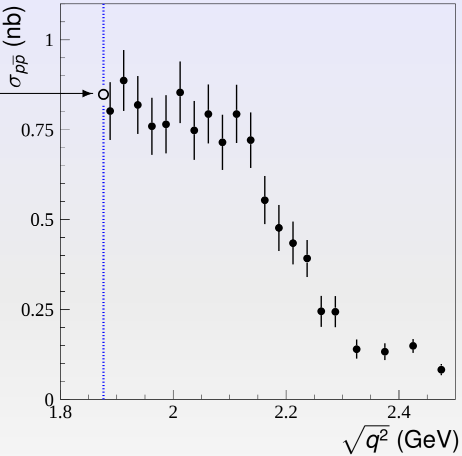

At the threshold

$$\sigma_{p\bar{p}}(4M_p^2) = \frac{\pi^2\alpha^3}{2M_p^2}\frac{\beta_p}{\beta_p}|G_S^p(4M_p^2)|^2$$

$$\sigma_{p\bar{p}}(4M_p^2) = 0.85\,|G_S^p(4M_p^2)|^2 \text{ nb}$$

$\Longrightarrow$

$|G_S^p(4M_p^2)| \equiv 1$

as pointlike fermion pairs!

BaBar: $|G_E^p|/|G_M^p|$ and $\sigma(e^+e^- \to p\bar{p})$

[PRD73, 012005]

Extracting $|G_S^p|$ and $|G_D^p|$ using

- data on $\sigma_{p\bar{p}}$
- data on $|G_E^p|/|G_M^p|$
- G_E^p/G_M^p phase $\phi \simeq 0$

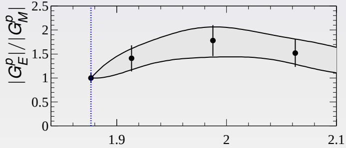

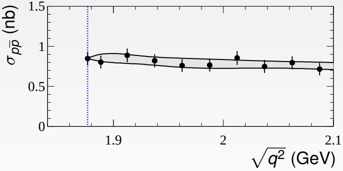

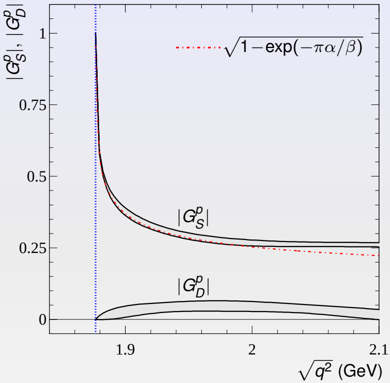

- $|G_S^p| \simeq \sqrt{1-\exp(-\pi\alpha/\beta)}$
- **No need of resummation factor?**

$e^+e^- \to n\bar{n}$

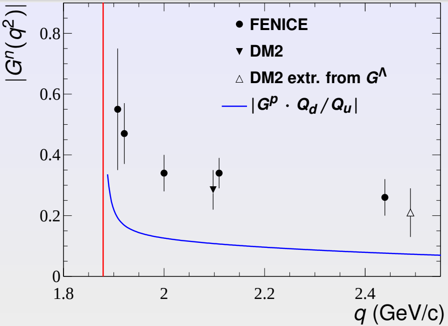

- Measured only once by FENICE at ADONE
- $\int\mathcal{L} = 500\ \text{nb}^{-1}$ (15' at BESIII)
- $\sim$ 100 candidates $n\bar{n}$ events!
- $\sigma(n\bar{n}) > \sigma(p\bar{p})$?
- Not zero at threshold?

BESIII has the unique possibility to measure this cross section

- $J/\Psi \to n\bar{n}$ (BR $\simeq 2 \cdot 10^{-3}$) $\geq 10^4$ events
- $\Psi(2S) \to n\bar{n}$ (BR $\simeq 3 \cdot 10^{-4}$) $\geq 10^3$ events
- At threshold by means of ISR (boost)
- n, $\bar{n}$ detection efficiency and pattern by means of: $J/\Psi \to n(\bar{p}\pi^+)$ and $J/\Psi \to \bar{n}(p\pi^-)$ ($\geq 10^5$ events)

$e^+e^- \to n\bar{n}$: preliminary from SND

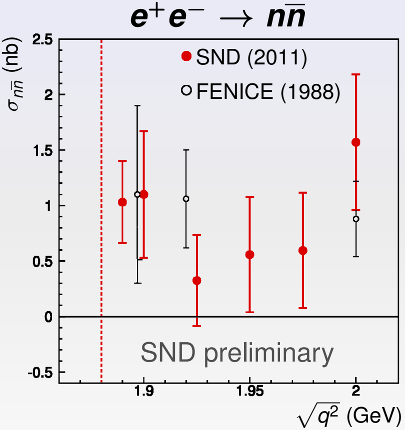

- **Scan 2011**
- **Maximum energy: 2 GeV**
- **Efficiency $\sim$ 30%**
- **Above $n\bar{n}$ threshold:** $\sigma_{n\bar{n}} = 0.8 \pm 0.2$ **nb**

$p\bar{p}$ and $n\bar{n}$ data from **BESIII**

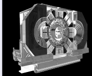

- **One year of data taking:** $T = 1.5 \times 10^7$ s
- **Average luminosity:** $\overline{\mathcal{L}} = 3 \times 10^{32}$ cm^{-2}s^{-1}
- **Center of mass energy:** $E_{c.m.} = 3.77$ GeV
- **Detection efficiences:** $\epsilon_{n\bar{n}} = 0.4$ $\epsilon_{p\bar{p}} = 0.8$
- **Number of events:** $N_{n\bar{n}} \simeq 1000$ $N_{p\bar{p}} \simeq 2000$

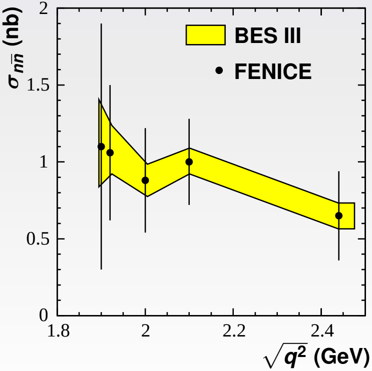

J/Ψ strong and electromagnetic phase

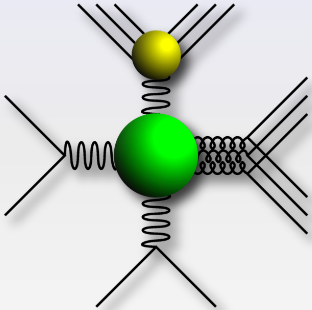

J/Ψ strong and electromagnetic decay amplitudes

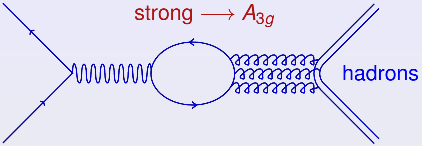

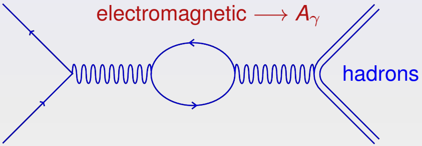

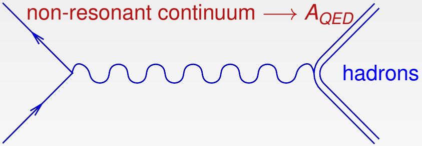

Resonant contributions

$$\Phi_p(G_p^M) \sim \Phi_\gamma \qquad \Phi_{3g} = 0$$

$$\Phi_\gamma\text{: relative } A_{3g} - A_p$$

- $J/\Psi \to N\bar{N}$ $\quad \Phi_p = 89^\circ \pm 15^\circ$ [1]
- $J/\Psi \to VP\ (1^-0^-)$ $\quad \Phi_p = 106^\circ \pm 10^\circ$ [2]
- $J/\Psi \to PP\ (0^-0^-)$ $\quad \Phi_p = 89.6^\circ \pm 9.9^\circ$ [3]
- $J/\Psi \to VV\ (1^-1^-)$ $\quad \Phi_p = 138^\circ \pm 37^\circ$ [3]

NO INTERFERENCE!

Non-resonant continuum

- affects the measured BR [4]
- affects Φ_p [4]

INTERFERENCE WITH A_{3g}!

[1] R. Baldini, C. Bini, E. Luppi, Phys. Lett. B404, 362 (1997); R. Baldini et al., Phys. Lett. B444, 111 (1998).
[2] L. Kopke and N. Wermes, Phys. Rep. 174, 67 (1989); J. Jousset et al., Phys. Rev. D41,1389 (1990).
[3] M. Suzuki et al., Phys. Rev. D60, 051501 (1999).
[4] P. Wang, arXiv:hep-ph/0410028v2 and references therein.

J/Ψ strong and electromagnetic decay amplitudes

IMAGINARY AMPLITUDES HARD TO BE EXPLAINED!

- $J/\Psi \subset$ perturbative regime ($\longleftarrow \Gamma_{J/\Psi} \sim 93 KeV$)
- pQCD $\longrightarrow$ real A_γ, A_{3g}
- QCD does not provide sizeable imaginary amplitudes (Φ_p 10° at most [1])
- a $J/\Psi - V$ glueball mixing [2] may explain imaginary amplitudes; and $\Psi(2S)$?
- determination of phases Φ_p rely on theoretical hypotheses

EXPERIMENTAL DATA

- no interference term in the inclusive J/Ψ and $\Psi(2S)$ production
- early evidence of an interf. term in $e^+e^- \to J/\Psi \to \mu^+\mu^-$ @ SLAC [3]
- no clear evidence of interf. or glueball in $e^+e^- \to J/\Psi \to \rho\pi$ @ BESII [4]

[1] J. Bolz and P. Kroll, WU B 95-35.
[2] S.J. Brodsky, G.P. Lepage, S.F. Tuan, Phys. Rev. Lett. 59, 621 (1987).

Simulated $e^+e^- \to N\bar{N}$ @ $s \sim M^2_{J/\Psi}$

interference must have opposite sign as magnetic moments

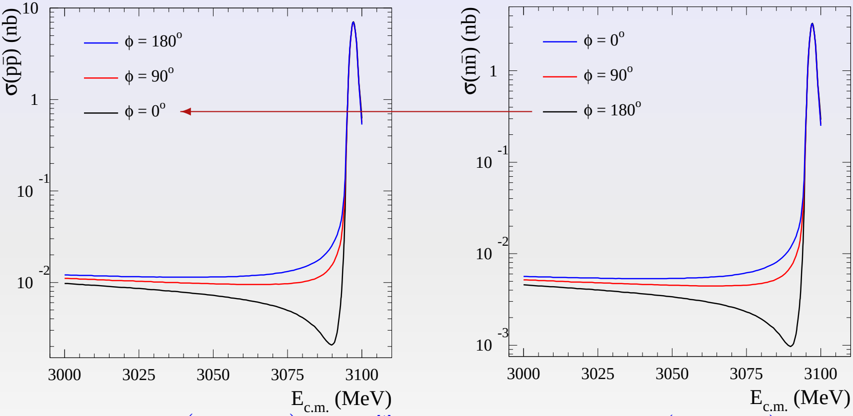

continuum reference: $\sigma\left(e^+e^- \to p\bar{p}\right) \sim 11\ pb$ [1]

continuum reference: $\sigma\left(e^+e^- \to n\bar{n}\right) \sim 5\ pb$ [1,2]

radiative corrections and beam energy spread (BESIII) included!

[1] B. Aubert et al. [BABAR Collaboration], Phys. Rev. D 73, 012005 (2006).
[2] R. Baldini, S. Pacetti, A. Zallo, arxiv:0812.3283 [hep-ph].

Simulated $e^+e^- \to p\bar{p}$ @ $s \sim M^2_{J/\psi}$ - **BESIII** scenario

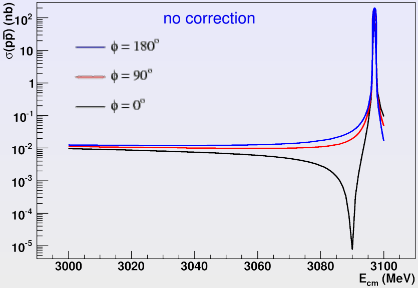

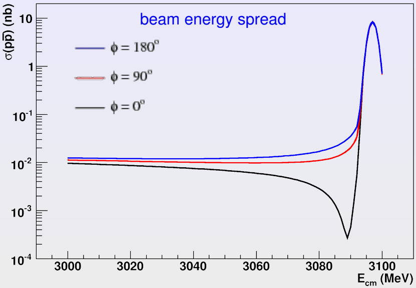

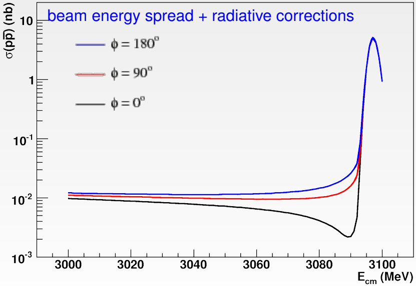

CORRECTIONS NEEDED!

- small effects from beam energy spread
- significant suppression from radiative corrections

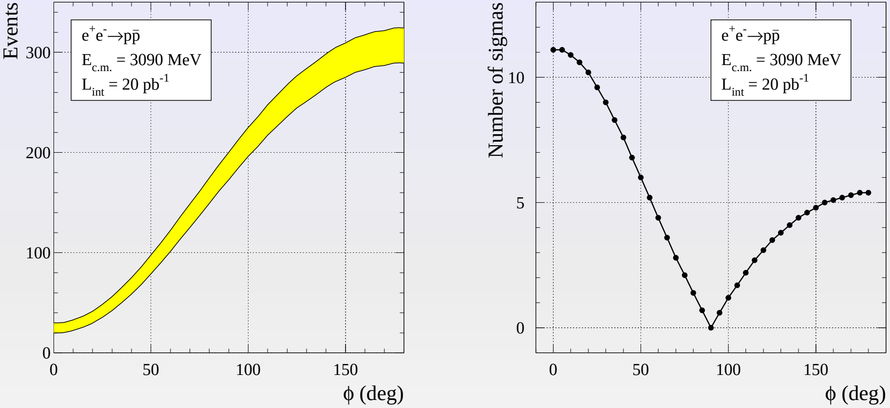

continuum reference: $\sigma\,(e^+e^- \to p\bar{p}) \sim 11\ pb$ [1]

radiative corrections and beam energy spread (BESIII) included!

[1] B. Aubert et al. [BABAR Collaboration], Phys. Rev. D 73, 012005 (2006).

Simulated $e^+e^- \to n\bar{n}$ @ $s \sim M^2_{J/\psi}$ (20 pb^{-1})

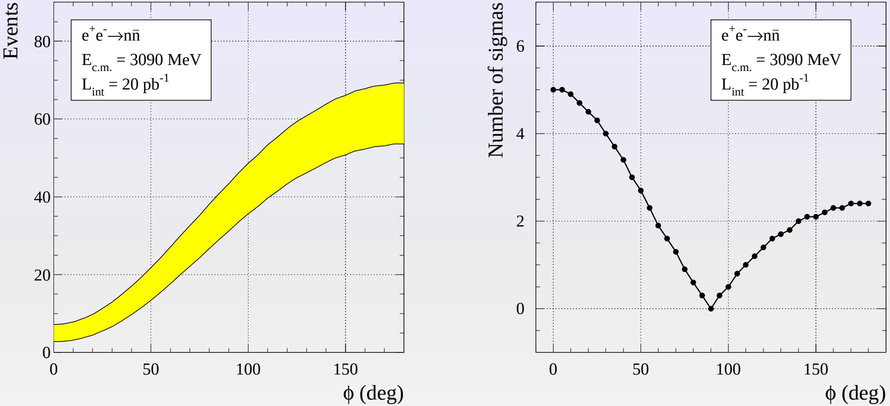

continuum reference: $\sigma\,(e^+e^- \to n\bar{n}) \sim 5\ pb$ [1,2]

radiative corrections and beam energy spread (BESIII) included!

[1] B. Aubert et al. [BABAR Collaboration], Phys. Rev. D 73, 012005 (2006).
[2] R. Baldini, S. Pacetti, A. Zallo, hep-ph0812.328v2.

2012 J/Ψ line shape scan at **BESIII**

Energy selection depends on the process

- 2 points at low $\sqrt{s}$:
  - fix continuum
  - fix slope
- 2 points at the deep
- 1 point at resonance raise

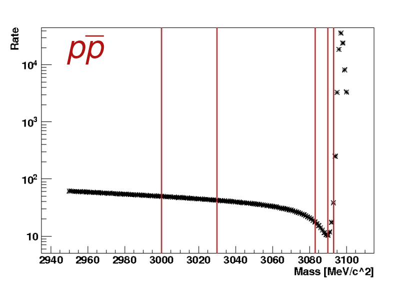

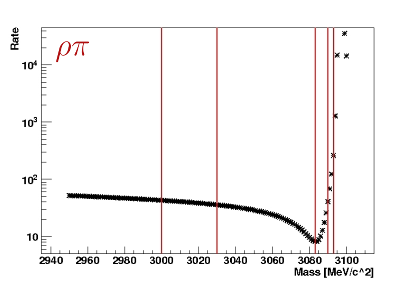

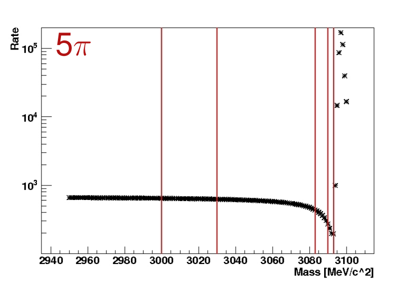

2012 J/Ψ line shape scan at **BESIII**

Energy requested $[MeV]$	Energy collected $[MeV]$	L_{int} $[pb^{-1}]$
3050	3046	14.0
3060	3056	14.0
3083	3086	16.5
3090	3085	14.0
3093	3088	14.0
3097	3097	79.6

Analysis in progress!

Measurement of $J/\Psi \to p\bar{p}$, $n\bar{n}$

- dominant strong amplitude: $|A^N_{3g}| > |A^N_\gamma|$
- isospin symmetry $\to |A^p_{3g}| = |A^n_{3g}|$
- $A^p_\gamma = -A^n_\gamma$ as magnetic moments
- assuming pQCD: Im $A^N_{3g} \sim 0$

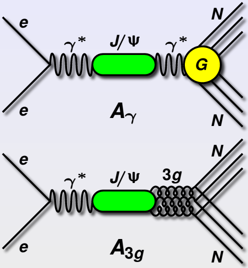

$$\frac{B(J/\Psi \to n\bar{n})}{B(J/\Psi \to p\bar{p})} = \left|\frac{A^n_{3g} + A^n_\gamma}{A^p_{3g} + A^p_\gamma}\right|^2 \sim 2$$

- BESII at BEPC [PLB591,42]: $B(J/\Psi \to p\bar{p}) = (2.26 \pm 0.01 \pm 0.14) \times 10^{-3}$
- FENICE at ADONE [PLB444,111]: $B(J/\Psi \to n\bar{n}) = (2.2 \pm 0.4) \times 10^{-3}$

$$B(J/\Psi \to p\bar{p}) \simeq B(J/\Psi \to n\bar{n})$$

$$\Downarrow$$

large $A^N_{3g} - A^N_\gamma$ relative phase

BESIII results: $J/\Psi \rightarrow p\bar{p}, n\bar{n}$

PRD86,032014(12)

$n\bar{n}$ identification

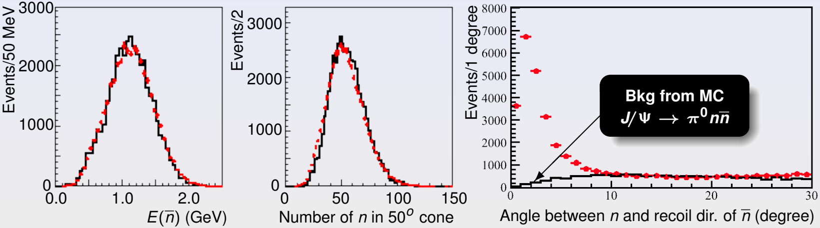

BESIII

$$B(J/\Psi \rightarrow n\bar{n}) = (2.07 \pm 0.01 \pm 0.17) \cdot 10^{-3}$$

$$B(J/\Psi \rightarrow p\bar{p}) = (2.112 \pm 0.004 \pm 0.031) \cdot 10^{-3}$$

PDG

$$B(J/\Psi \rightarrow n\bar{n}) = (2.2 \pm 0.4) \cdot 10^{-3}$$

$$B(J/\Psi \rightarrow p\bar{p}) = (2.17 \pm 0.07) \cdot 10^{-3}$$

$$\Phi = (88.7 \pm 8.1)^\circ$$

large phase between strong and e.m. amplitudes!

Conclusions and Perspectives with BESIII

- Asymptotic behavior not well understood
- Pointlike behavior not only at threshold
- Sommerfeld resummation factor needed?
- Neutral baryons puzzle

- More precise data on $\sigma_{p\bar{p}}$ above 3 GeV allow:
  - accurate study of the step around 3 GeV
  - precise measurement of the ratio $|G_E^p|/|G_M^p|$
- Unique possibility to measure the $n\bar{n}$ cross section thanks to ISR and scan
- Measurement of the relative phase between e.m. and strong amplitudes in $J/\Psi \to N\bar{N}$ decays
- First BESIII results confirm a large phase scenario and considerably improve PDG data on $J/\Psi \to N\bar{N}$.

BACK-UP SLIDES

BESIII main features

Drift Chamnber

- Low gas misture (60% He, 40% Propane)
- Carbon filter cylindres: $R_{\rm in} = 6.3$ cm, $T_{\rm in} = 1$ mm,
  $R_{\rm out} = 81$ cm $T_{\rm out} = 1$ cm
- 6 Al stepped flanges: T = 1.8 cm
- 43 layers: 7000 25 μm gold-plated sense wires, 22000 Al field-shaping wires
- $\sigma_{x,y} \sim 130\ \mu$m, $\sigma(De/dx) \sim 6\%$

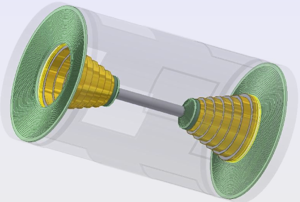

CsI Calorimeter

- 6240 CsI(Tl): 5280 Barrel, 960 Endcaps, 13000 photodiodes
- 28×5.2^2 cm^3
- $\Delta E/E \sim 2.5\%$ at 1 GeV, noise ~ 220 keV

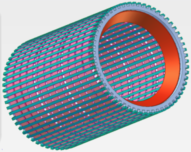

Superconducting Magnet: 1 T

RPC μ Chambers

9/8 layers Barrel/Endcaps, Strip x, y 4cm
Plastic foil instead linseed oil: noise ~ 0.1 Hz/cm^2, $\epsilon \sim 95\%$

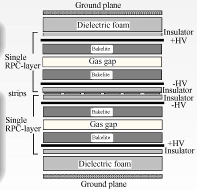

Space-like G_E^p / G_M^p measurements

Space-like data

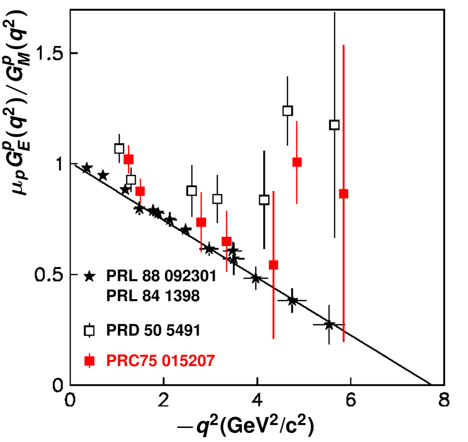

$$G_E^p = F_1^p + \frac{q^2}{4M_p^2} F_2^p$$

$$G_M^p = F_1^p + F_2^p$$

Space-like

F_1 and $\frac{q^2}{4M_p^2} F_2$ cancellation

$$\frac{G_E^p(q^2)}{G_M^p(q^2)} < 1$$

Time-like

F_1 and $\frac{q^2}{4M_p^2} F_2$ enhancement

$$\left| \frac{G_E^p(q^2)}{G_M^p(q^2)} \right| > 1$$

Rosenbluth separation

SP PR79,615

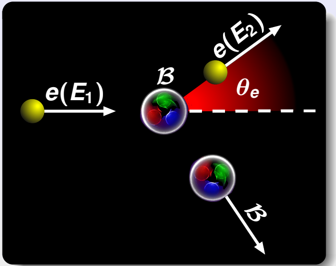

Rosenbluth formula

$$\frac{d\sigma}{d\Omega} = \left(\frac{d\sigma}{d\Omega}\right)_{\rm Mott} \frac{1}{1-\tau}\left[G_E^2 - \frac{\tau}{\epsilon} G_M^2\right] \qquad \tau = \frac{q^2}{4M_N^2}$$

- Mott pointlike cross section

$$\left(\frac{d\sigma}{d\Omega}\right)_{\rm Mott} = \frac{4\alpha^2}{(-q^2)^2}\frac{E_2^3}{E_1}\cos^2(\theta_e/2)$$

- Photon polarization

$$\epsilon = \left[1 + 2\,(1-\tau)\tan^2(\theta_e/2)\right]^{-1}$$

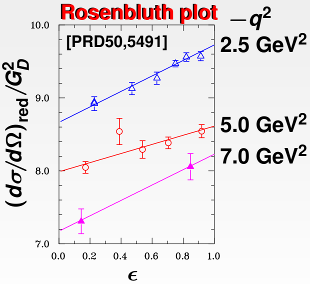

Reduced cross section

$$\left(\frac{d\sigma}{d\Omega}\right)_{\rm red} = \frac{\epsilon(1-\tau)}{\tau}\frac{(d\sigma/d\Omega)_{\rm exp}}{(d\sigma/d\Omega)_{\rm Mott}} = G_M^2 - \frac{\epsilon}{\tau}G_E^2$$

- $(d\sigma/d\Omega)_{\rm red}\,(\epsilon)$ slope $\longrightarrow G_E$
- $(d\sigma/d\Omega)_{\rm red}\,(\epsilon)$ intercept $\longrightarrow G_M$

Sachs form factors G_E and G_M are extracted from Born cross sections (one-γ exchange)

The Born term is obtained from experimental cross sections correcting for radiative effects

$$\frac{d\sigma^{\text{exp}}}{d\Omega} = (1+\delta)\frac{d\sigma^{\text{Born}}}{d\Omega}$$

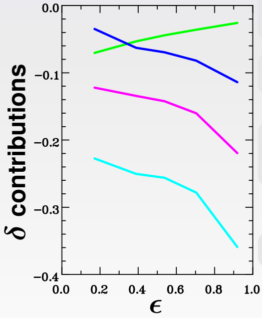

proton side + two-photon

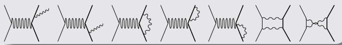

Apparatus corrections [PRD50,5491(94)]

electron side

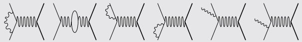

Total correction

δ depends on ϵ

$\Downarrow$

It affects the slope in Rosenbluth plot

Polarization observables

A.I. Akhiezer, M.P. Rekalo, Sov. Phys. Dokl. 13, 572 (1968)

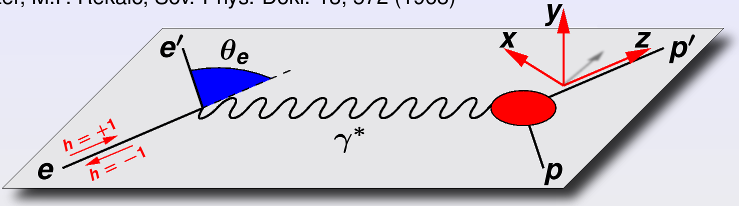

- Elastic scattering of longitudinally polarized ($h = \pm 1$) electrons on nucleon target
- Hadronic tensor: $W_{\mu\nu} = \underbrace{W_{\mu\nu}(0)}_{\text{no pol.}} + \underbrace{W_{\mu\nu}(\vec{P}) + W_{\mu\nu}(\vec{P}')}_{\text{ini. or fin. pol. of } N} + \underbrace{W_{\mu\nu}(\vec{P}, \vec{P}')}_{\text{ini. and fin. pol. of } N}$
- In case of polarized ($h = \pm 1$) electrons on unpolarized nucleon target:

$$P'_x = -\frac{2\sqrt{\tau(\tau-1)}}{G_E^2 - \frac{\tau}{\epsilon} G_M^2} G_E G_M \tan\left(\frac{\theta_e}{2}\right)$$

$$P'_z = \frac{(E_e + E'_e)\sqrt{\tau(\tau-1)}}{M\left(G_E^2 - \frac{\tau}{\epsilon} G_M^2\right)} G_M^2 \tan^2\left(\frac{\theta_e}{2}\right)$$

$$\frac{P'_x}{P'_z} = -\frac{2M\cot(\theta_e/2)}{E_e + E'_e} \frac{G_E}{G_M}$$

Neutral Baryons puzzle (*BABAR*)

PRD76, 092006

$$\sigma(e^+e^- \to \mathcal{B}^0\overline{\mathcal{B}}^0) = \frac{4\pi\alpha^2\beta C_0}{3q^2}\left[|G_M^{\mathcal{B}^0}|^2 + \frac{2M^2_{\mathcal{B}^0}}{q^2}|G_E^{\mathcal{B}^0}|^2\right] \xrightarrow[q\to 2M_{\mathcal{B}^0}]{} \frac{\pi\alpha^2\beta}{2M^2_{\mathcal{B}^0}}|G^{\mathcal{B}^0}|^2 \to 0$$

No Coulomb correction at hadron level: $C_0 = 1$

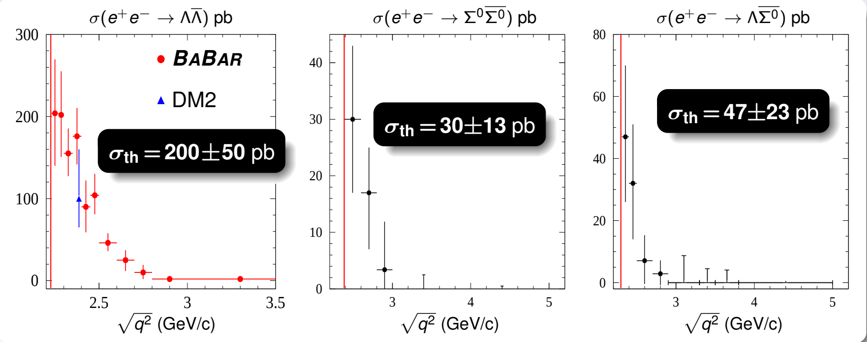

Remnant of Coulomb interactions at quark level? $\Rightarrow$ $C_0 \propto \beta^{-1}$ as $q \to 2M_{\mathcal{B}^0}$ $\Rightarrow$ For any neutral baryon

$$\sqrt{\sigma_{\mathcal{B}^0\overline{\mathcal{B}}^0}} \propto \frac{|G^{\mathcal{B}^0}|}{M_{\mathcal{B}^0}}$$

Baryon octet and U-spin

arXiv:0812.3283

Coulomb correction at quark level

$$\sqrt{\sigma_{\mathcal{B}^0\overline{\mathcal{B}}^0}(4M^2_{\mathcal{B}^0})} = K \cdot \frac{|G^{\mathcal{B}^0}|}{M_{\mathcal{B}^0}}$$

K is unknown but equal for all neutral baryons with equal quark content

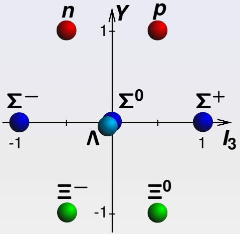

$$(Y, I_3) \to (Y_U, U_3)$$

$$U_3 = -\tfrac{1}{2} I_3 + \tfrac{3}{4} Y$$

$$Y_U = -Q$$

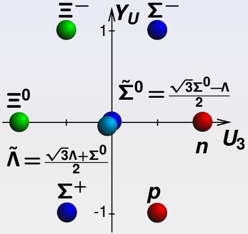

Indirect relation: $G^{\Sigma^0} - G^{\Lambda} + \frac{2}{\sqrt{3}} G^{\Lambda\Sigma^0} = 0$

$$M_{\Sigma^0}\sqrt{\sigma_{\Sigma^0\overline{\Sigma^0}}} - M_{\Lambda}\sqrt{\sigma_{\Lambda\overline{\Lambda}}} + \frac{2}{\sqrt{3}}\overline{M_{\Lambda\Sigma^0}}\sqrt{\sigma_{\Lambda\overline{\Sigma^0}}} = (-0.06 \pm 6.0) \times 10^{-4}$$

Baryon octet and U-spin

Coulomb correction at quark level

$$\sqrt{\sigma_{\mathcal{B}^0\overline{\mathcal{B}^0}}(4M^2_{\mathcal{B}^0})} = K \cdot \frac{|G^{\mathcal{B}^0}|}{M_{\mathcal{B}^0}}$$

K is unknown but equal for all neutral baryons with equal quark content

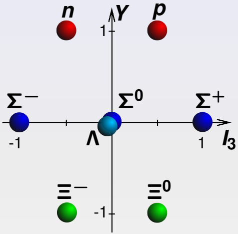

$$(Y, I_3) \to (Y_U, U_3)$$

$$U_3 = -\frac{1}{2} I_3 + \frac{3}{4} Y$$

$$Y_U = -Q$$

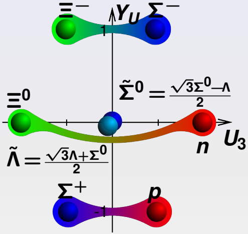

Indirect relation: $G^{\Sigma^0} - G^{\Lambda} + \frac{2}{\sqrt{3}} G^{\Lambda\Sigma^0} = 0$

$$M_{\Sigma^0}\sqrt{\sigma_{\Sigma^0\overline{\Sigma^0}}} - M_\Lambda\sqrt{\sigma_{\Lambda\overline{\Lambda}}} + \frac{2}{\sqrt{3}}\overline{M_{\Lambda\Sigma^0}}\sqrt{\sigma_{\Lambda\overline{\Sigma^0}}} = (-0.06 \pm 6.0) \times 10^{-4}$$

Data and U-spin predictions at threshold

- $M_{\Sigma^0}\sqrt{\sigma_{\Sigma^0\overline{\Sigma^0}}} - M_\Lambda\sqrt{\sigma_{\Lambda\bar\Lambda}} + \frac{2}{\sqrt{3}}\overline{M_{\Lambda\Sigma^0}}\sqrt{\sigma_{\Lambda\Sigma^0}} = (-0.06 \pm 6.0)\times 10^{-4}$
- $\sigma(e^+e^- \to n\bar n) = \frac{1}{4}(3\sqrt{\sigma_{\Lambda\bar\Lambda}}M_\Lambda - \sqrt{\sigma_{\Sigma^0\overline{\Sigma^0}}}M_\Sigma)^2\frac{1}{M_n^2} = 0.5 \pm 0.2$ nb

$e^+e^- \to n\bar n$ **(FENICE@ADONE)**

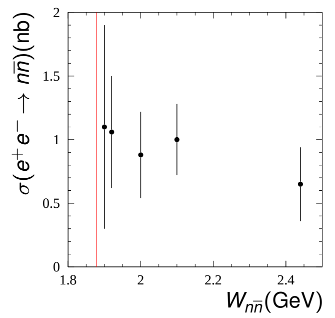

BABAR: integrated Sommerfeld factor and G^p_{eff}

$$|G^p_{\text{eff}}|^2 = \frac{\sigma_{p\bar{p}}(q^2)}{\mathcal{C}\,\frac{16\pi\alpha^2}{3}\,\frac{\sqrt{1-1/\tau}}{4q^2}\left(1+\frac{1}{2\tau}\right)}$$

$$|G^p_{\text{no-sum}}|^2 = \frac{\sigma_{p\bar{p}}(q^2)}{\mathcal{E}\,\frac{16\pi\alpha^2}{3}\,\frac{\sqrt{1-1/\tau}}{4q^2}\left(1+\frac{1}{2\tau}\right)}$$

$$\overline{\mathcal{R}^{-1}} = \frac{1}{\Delta q}\int_0^{\Delta q}\left[1-e^{-\frac{\pi\alpha}{\beta}}\right]d\sqrt{q^2}$$

$$\Delta q = \sqrt{q^2} - 2M_p$$

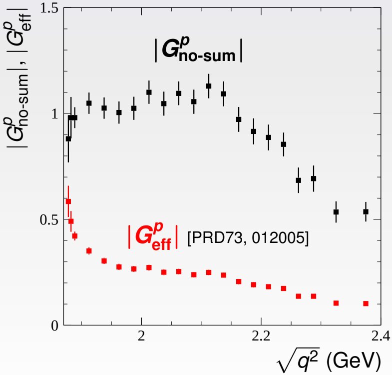

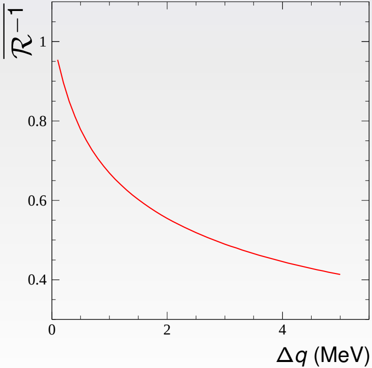

J/Ψ strong and electromagnetic decay amplitudes

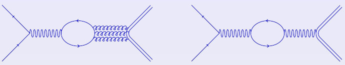

resonant

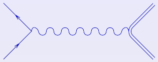

non resonant

$$x = \frac{M_{J/\Psi} - \sqrt{s}}{\Gamma_{TOT}/2} \quad A_R = \alpha\left(\frac{x}{1+x^2} + i\frac{1}{1+x^2}\right)$$

$$\Phi_\alpha = \arctan\frac{|A_\gamma|\sin\Phi_p}{|A_{3g}| + |A_\gamma|\cos\Phi_p}$$

$$\Phi_{A_\gamma} \sim \Phi_p = \Phi_{G_p^M} \quad A_{NR} = -\beta e^{i\Phi_p}$$

$$\beta = \sqrt{\sigma\,(e^+e^- \Leftrightarrow p\bar{p})}$$

G_p^M real @ $W \sim M_{J/\Psi}$ [1]

$$\Delta\Phi = \Phi_p - \Phi_\alpha \sim \Phi_p$$

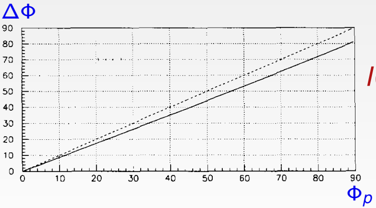

$$I(x) = |A_R + A_{NR}|^2$$
$$= \frac{\alpha^2}{1+x^2} + \beta^2 - \frac{2\beta\alpha}{1+x^2}\left(x\cos\Delta\Phi + \sin\Delta\Phi\right)$$

[1] S.J. Brodsky, G.P. Lepage, S.F. Tuan, Phys. Rev. Lett. 59, 621 (1987).

Early evidence of interference in $e^+e^- \to \mu^+\mu^-$

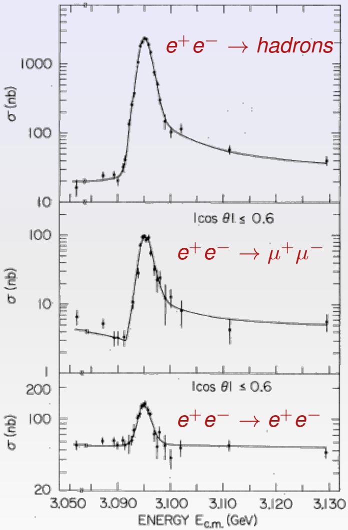

J/Ψ production
@ SPEAR (SLAC) [1]

[1] R. Baldini, C. Bini, E. Luppi, Phys. Lett. B404, 362 (1997).

Simulated $e^+e^- \to p\bar{p}$ @ $s \sim M^2_{J/\psi}$ ($20\ pb^{-1}$)

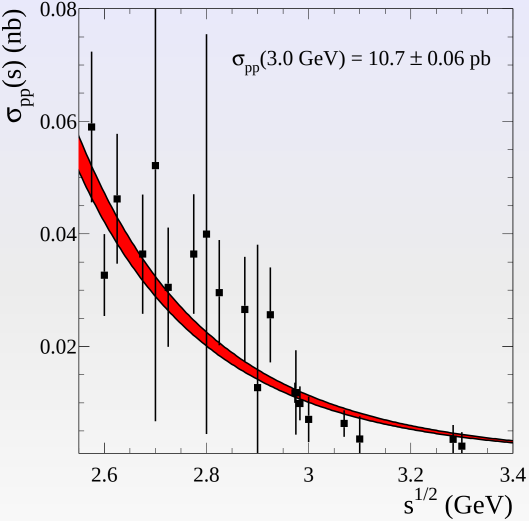

[1] B. Aubert et al. [BABAR Collaboration], Phys. Rev. D 73, 012005 (2006).